# The Laser Driven Particle Accelerator Project: Theory and Experiment

T. Plettner*, J.E. Spencer†, Y.C. Huang††, R.L Byer*, R.H. Siemann†, and T.I. Smith‡

*Department of Applied Physic, and ‡Hansen Experimental Physics Laboratory, Stanford University, Stanford, CA 94305.
†Stanford Linear Accelerator Center, Stanford, CA 94309.
††Department of Atomic Science, National Tsing-Hua University,Taiwan 30043

**Abstract**. A proof of principle experiment for laser driven electron acceleration from crossed laser beams in a dielectric loaded vacuum is being carried out at Stanford University. We seek to measure a maximum energy gain of about 250 keV for a 30-35 MeV electron beam in one accelerator cell. We use laser pulses of a few picoseconds of duration from a regenerative Ti:sapphire laser amplifier at a wavelength of 800 nm in a laser-electron interaction distance of ~ 1 mm.

## MOTIVATION

The rapid development of laser technology has made it possible to produce sub-picosecond pulses with fields in excess of $10^{10}$ V/m at wavelengths of the order of 1 μm with commercial table top lasers. At these wavelengths and pulse durations dielectric materials can tolerate very intense fields. A 1 psec pulse of 1053 nm light on a $SiO_2$ has been measured to have a damage threshold of ~ 2J/cm$^2$, equivalent to about $10^{10}$ V/m (1). Fields of this magnitude could produce an average gradient of about 1 GeV/m in a suitably designed dielectric based accelerator structure.

## THE EXPERIMENT

### The site

The experiment is carried out at the SCA-FEL center at Stanford University because this facility is capable of providing a low energy spread beam (50-100 keV). It has an energy of 35 MeV and consists of 1 psec bunches that contain ~$10^8$ electrons. A high peak power Ti:sapphire laser system is also available there. The experiment is located downstream from an FEL. In order to avoid a large background from unwanted electron bunches the experiment is placed in a separate line. A fast deflector located in the main line selects the bunch that is timed with the laser. Fig. 1 shows the basic layout of the experiment at the SCA-FEL center.

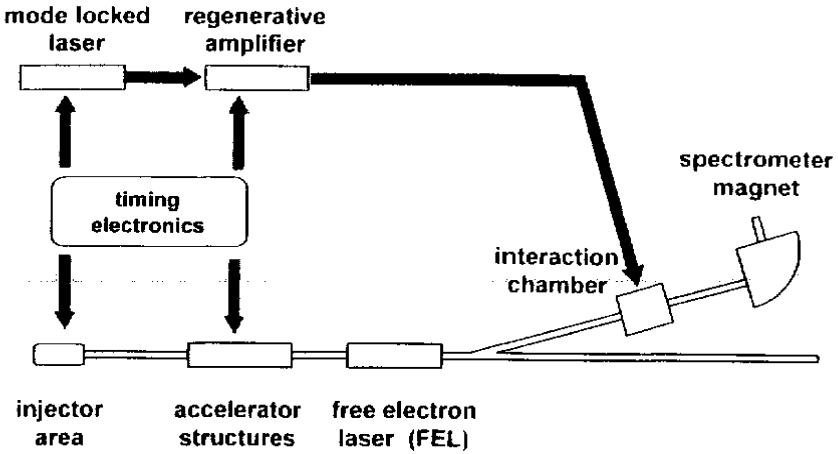


**FIGURE 1**. Diagram of the experiment

The accelerator cell is located inside the interaction chamber and any change in energy produced in the cell is measured with a high resolution spectrometer magnet located downstream.

### The energy spectrometer and some aspects of the beam

The energy spectrometer is a dipole sector magnet designed to bend the beam by 90 degrees in a radius of ~1/2 m. Its first order resolving power $R$ has been determined to be

$$R = \sqrt{\left\langle \frac{P}{\Delta P} \right\rangle^2} = \frac{\eta_x}{\sigma_x} = \frac{1.12 \quad m}{30 \quad \mu m} = 4 \cdot 10^4 \qquad (1)$$

where $\eta_x$ is the dispersion and $\sigma_x$ is the monochromatic spot size at the focal plane. At 30 MeV this would correspond to an energy resolution of 750 eV, but due to the much larger initial energy spread of the beam the effective energy resolution is the initial energy spread of the beam itself: about 50 keV. The FEL has a detrimental effect on the energy spread of the beam. Fig. 2 shows this effect clearly. The deflector has to be

CP472, *Advanced Accelerator Concepts Eighth Workshop*,
edited by W. Lawson, C. Bellamy, and D. Brosius

timed such that it selects an electron bunch that passed through the wiggler when no FEL action was present in order to obtain a narrow energy spread pulse for the experiment.

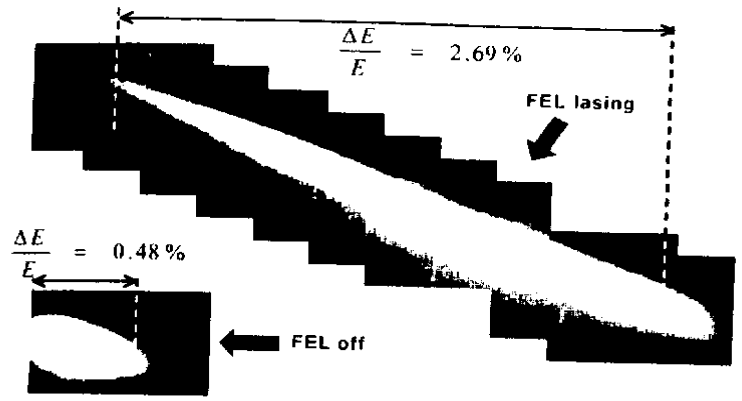


**FIGURE 2.** Effect of the FEL action on the electron beam

## The accelerator cell

The accelerator cell consists of a set of four fused silica prisms with a dielectric high reflecting coating on their surface. One pair of prisms is used to couple the pair of laser beams into the cell and the other pair of prisms takes the laser beams out. The gap between the prisms in each pair is the slit that allows the electron beam to transverse the cell. Fig. 3 shows a perspective view of the cell.

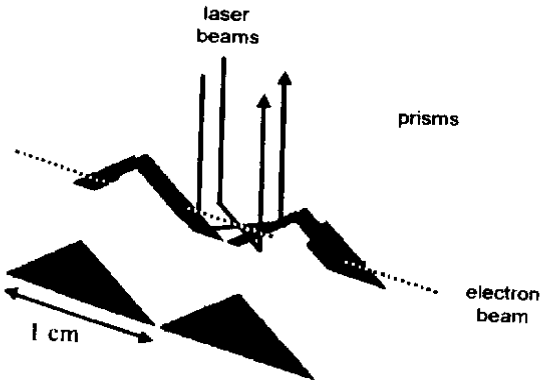


**FIGURE 3** The accelerator cell



## ANALYSIS

A pair of properly phased crossed laser beams yields an interference pattern that at certain regions produces an electric field oriented half way between the crossing laser beams. For small angles of crossing between the laser beams this effective longitudinal field travels at a phase velocity which is close enough to the speed of light so that a beam of particles with a large $\gamma$ traveling in that direction sees a reasonably long slippage distance[1]. This acceleration scheme has been studied in the past (2,3) and possible accelerator structure designs have been proposed (4,5). The analytical expression for the longitudinal electric field $E_z$ seen by a particle travelling at the speed of light is given by

$$E_z(z,t) = -\frac{2E_0 \sin\theta}{\left(1+\hat{z}^2\cos^2\theta\right)^{1/2}} \cdot \exp\left[-\frac{(z/\theta_d)^2 \sin^2\theta}{\left(1+\hat{z}^2\cos^2\theta\right)}\right] \cdot \cos\psi_i$$

$$\psi_i = k \cdot z \cdot \cos\theta - \omega \cdot t + \frac{\hat{z}^3 \cos^3\theta \cdot \tan^2\theta}{\theta_d^2\left(1+\hat{z}^2\cos^2\theta\right)} - 2\tan^{-1}(\hat{z}\cos\theta) + \phi_0 \qquad (2)$$

where $\theta$ is the angle of crossing of the laser beam, $\theta_d$ the diffraction angle, $\omega$ the frequency of the laser, $\hat{z}$ the position (normalized to the Rayleigh range) of the particle down the axis of propagation, $k$ the wave vector and $\phi_0$ an arbitrary initial phase of the laser field. A diagram showing the electric fields and the corresponding $E_z$ field down the axis of propagation of the particles is shown in Fig. 4. Because of the phase velocity mismatch between the laser field and the particle $E_z$ shows an oscillatory behavior.

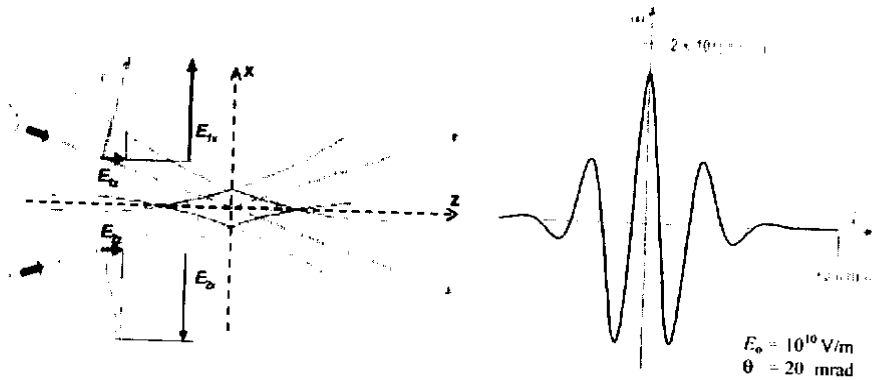


**FIGURE 4.** Illustration of the $E_z$ field generated from a pair of gaussian beams.

[1] the distance required for a particle beam to see a phase shift of $\pi$ in the phase of the electric field

By the Lawson-Woodward theorem (6) the particle gains no energy if it interacts with the laser field linearly over an infinite distance. Therefore to obtain a nonzero energy gain the particle-laser interaction distance has to be made finite by the use of an accelerator cell with suitable optical components to couple the light in and out of the path of the electron beam in a short enough distance. The energy gain in one cell of inner length $a$ is given by

$$U(a) = \int_{-a/2}^{+a/2} E_z(z) \cdot dz \qquad (3)$$

From equation (2) the energy gain depends on the length of the cell $a$, the angle of crossing of the laser beams $\theta$, their relative phase, their polarization and their intensity. Fig. 5 shows the effect of the length of the cell and the angle of crossing between the laser beams.

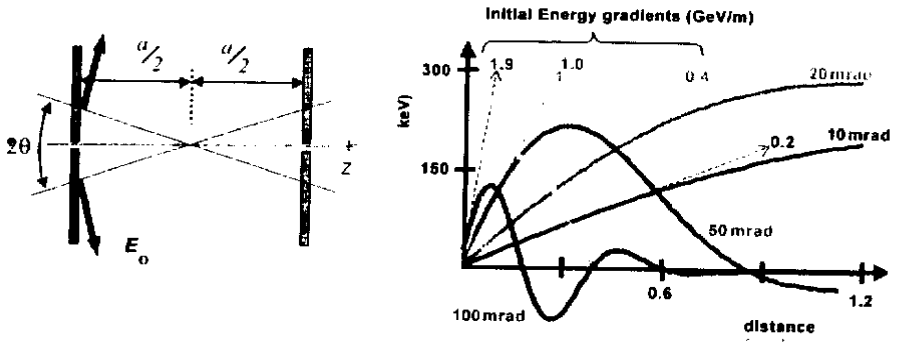


**FIGURE 5.** Schematic diagram of an accelerator cell and curves for Energy gain versus size of accelerator cell for various laser beam crossing angles

At steeper angles of crossing the laser beams create a larger effective longitudinal field larger and hence the initial gradient is higher. However the phase velocity mismatch between the laser and the particle beams is bigger and therefore slippage distance is decreased. This explains the large initial gradient and oscillatory behavior for the 100 mrad curve when compared to the 10 mrad curve in Fig. 5.

## EXPERIMENTAL CONSIDERATIONS

There are several non-ideal experimental conditions that affect the outcome of the experiment, and have to be taken into account in order to make the correct predictions for the acceleration. These factors are:



- low energy electron beam with a $\gamma$ of about 70
- significant initial energy spread
- the electron beam is not optically bunched
- ultra short laser pulses comparable to the e-beam bunch length
- effects caused by the slit of the accelerator cell

### finite $\gamma$ and initial energy spread

In Fig. 5 an infinite $\gamma$ was assumed. For a low energy electron beam the slippage distance is reduced further. The effect is shown in Fig. 6. For an electron beam with an energy of ~35 MeV, laser beams crossing at 20 mrad and a cell 1 mm long the energy gain is reduced by about 30% when compared to that of a beam with infinite $\gamma$.

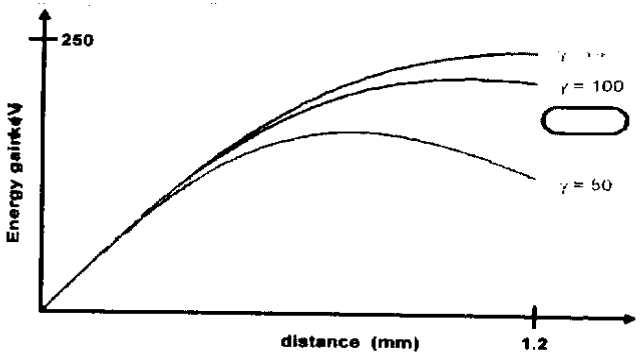


**FIGURE 6.** Effect of finite $\gamma$ on the energy. The circled value corresponds to the approximate energy of the electron beam used in this experiment

### Effect of initial energy spread and of no optical bunching

The previous graphs were obtained from single particle calculations that assumed the optimum phase of the laser beams for acceleration. The electron beam is not optically bunched and therefore it will see all the phases of the optical field. Hence an energy distribution showing accelerated as well as decelerated electrons is expected. Fig. 7 shows the predicted energy profiles at the exit of the accelerator cell for different input energy spreads of the electron beam for a time independent optical field. Assuming an equal distribution of mono energetic electrons with energy E over all phases of the laser field of constant laser intensity an energy distribution $I(U\text{-}E)$ for

the electron beam can be calculated. For a particular initial energy spread $S(E)$ of the beam the expected histogram $H(E)$ is the convolution of $S(E)$ and $I(E)$.

$$H(E) = \int_0^\infty S(E') \cdot I(E - E') \cdot dE' \qquad (4)$$

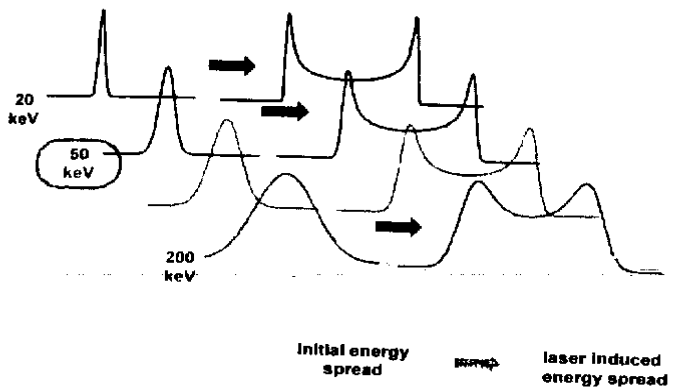


**FIGURE 7.** Energy profile of the e-beam at the exit of the accelerator cell. Energy spreads for single electron beam bunches below 50 keV have been observed.

The laser beam pulses have a time duration comparable to the e-beam bunches, and as Fig. 8 illustrates the energy profile is strongly dependent on the relative time duration between the e-beam and the laser beam.

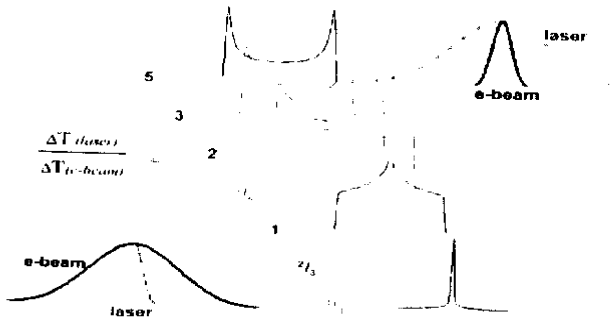


**FIGURE 8.** Effect of a finite laser pulse on the energy profile of the e-beam.



## Effect of the slit of the accelerator cell

In order to prevent the electron beam from travelling through matter a slit has to be built into the accelerator cell. A slit of a few microns is already larger than the wavelength of the laser field and hence diffraction effects due to the slit have to be considered. At the entrance and the exit of the accelerator cell some light leaks out of the cell. The leaking field at the entrance decreases the acceleration field inside the accelerator cell, while that at the exit removes some energy from the electrons. The net effect is a reduction of the electron energy gain. Slit effects have been studied in a previous paper (7). A 4-μm slit is expected to reduce the energy gain by 17% and a 6μm slit by 40%. Hence very small slit widths are preferred in order to reduce the leakage field.

When the electrons traverse the slits, the impact of the electron self-field upon the dielectric boundaries causes transition radiation at the cost of electron kinetic energy. A high impact field may also cause dielectric damage. In an attempt to obtain first-order estimation, we model the propagating electron self-field as an optical pulse and calculate the reflected radiation energy as the electron energy loss. The maximum line charge density subjected to a 10 GV/m damage field and radiation loss = 10% energy gain is ~ $10^7$ electrons/mm for our design parameters.

## TIMING BETWEEN THE LASER AND THE ELECTRON BEAM

Relative timing between the laser beam and the electron beam to the picosecond level is essential for the success of the experiment. A timing monitor that produces an error signal that controls the timing of the laser is required. We are seeking a reliable method for timing that is non-destructive to the laser or the electron beam. Compton scattering is a very precise method for confirming spatial and temporal overlap between the two beams, however it cannot provide a signed error signal and hence is no useful timing monitor when the beams are not overlapped. Furthermore only a maximum of ~$10^3$ photons produced by the Compton can be expected in this experiment.

One simple coarse timing scheme involves the use of a photo detector and a separate electron beam detector. A 6 picosecond rise time photo detector that monitors the laser has been installed. For the electron beam we will test the performance of several different monitors for lowest timing jitter: a beam position monitor (BPM), a resonant RF cavity, transition radiation and a multi channel plate (MCP). In order to obtain a signed timing error signal an RF mixer multiplies the signals from the photo diode and from the e-beam monitor. Once the beams are timed with this coarse timing technique a blind search for the precise overlap of the two beams will be performed. To keep this range reasonably small we hope to find the scheme suitable to get a timing uncertainty below 100 psec. Figure 9 is a diagram for this method of coarse timing.

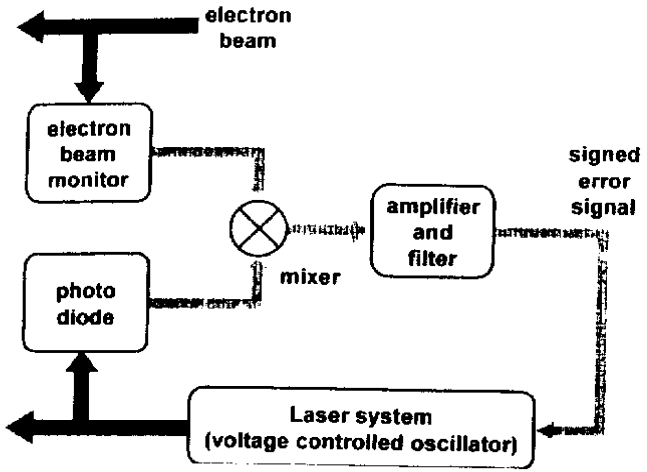


**FIGURE 9.** Block diagram of the coarse timing scheme

## SUMMARY

During the first year of the experiment the electron beam line and the laser beam transport line were installed. The energy spectrometer was tested and calibrated and furthermore we have achieved the ability to select single electron bunches and thus keep background noise levels low. Presently work is concentrated on finding a reliable scheme to synchronize the laser beam and the electron beam in order to overlap them in the accelerator cell. Once we have reliable method for achieving spatial and temporal overlap between the two beams we will attempt to confirm acceleration by measuring the change in the energy of the beam as a function of the various laser and accelerator cell parameters.

## ACKNOWLEDGEMENTS

The authors thank R. Route and M. Hennessy for their valuable help. This work is supported by the U.S. Department of Energy under the contract number DE-FG03-98ER41043.



## REFERENCES

1 Stuart, B.C. et al, Phys. Rev. Lett. **74**, 2248 (1995)
2 Haarland, C.M., *Optics Comm.* 114 (1995), pp 280-284
3 Sprangle, P., E. Esarey, J. Krall, A. Ting, *Optical Comm.* 124, 1996, pp. 69-73
4 Huang, Y.C., D. Zeng, W.M. Tulloch and R.L. Byer, Appl. Phys. Lett 68 (1996), pp 753-755
5 Huang, Y.C., R.L. Byer,, Appl. Phys. Lett. **69**, 2175 (1996).
6 Lawson, J.D., IEEE Trans. Nucl. Sci. **NS-26**, 4217 (1979). P.M. Woodward, J. IEE **93**, 1554 (1947)
7 Huang, Y.C. and R.L. Byer, to be published in *Rev. Sci. Ins.* July (1998).